Drying Technology, 29: 553–565, 2011

ISSN: 0737-3937 print/1532-2300 online
DOI: 10.1080/07373937.2010.507913

Taylor & Francis
Taylor & Francis Group

Characterization and Dehydration Behavior of a Natural, Ammonium Hydroxide, and Thermally Treated Zeolitic Tuff

G. Narin, D. Balköse, and S. Ülkü
Department of Chemical Engineering, Izmir Institute of Technology, Izmir, Turkey

Aqueous NH_4OH-treated and subsequently calcined forms of local natural zeolitic tuff were characterized by different techniques including scanning electron microscopy (SEM), X-ray powder diffraction, inductively coupled plasma–atomic emission spectroscopy (ICP-AES), volumetric N_2 adsorption at −196°C, thermogravimetry (TG), differential scanning calorimetry (DSC), and transmittance infrared spectroscopy. The dehydration behavior of the samples was investigated using an in situ temperature-programmed diffuse reflectance Fourier transform infrared spectroscopy (TP-DRIFTS) method under vacuum. The DRIFTS spectra recorded yielded information about the effect of the NH_4OH treatment and subsequent calcination on the dehydration behavior of the natural zeolite. Changes in the infrared bands corresponding to vibrations of the O−H and N−H bonds upon in situ heating under vacuum were analyzed.

Keywords Ammonium hydroxide treatment; Characterization; Clinoptilolite; Dehydration; DRIFTS

INTRODUCTION

Natural zeolites constitute a group of minerals having open aluminosilicate frameworks containing channels and cavities that accommodate cations and water molecules. Generally, these cations are exchangeable and the water molecules can be removed or replaced reversibly without disrupting the framework. The presence of water in the pores hinders adsorption of other molecules; thus adsorption and catalytic properties of zeolites are directly related to their water content. Water is adsorbed into zeolites by filling oxygen-lined channels and hydrating the cations present in the channels. The observed macroscopic thermal behavior of a zeolite depends on the type, amount, and position of the extraframework cations within the structure, their coordination to water molecules, their interactions with framework oxygen atoms, the presence of other water molecules, Si/Al ratio, time, temperature, pressure, and heating rate.

Dehydration behaviors of clinoptilolite have been investigated by various analytical techniques including thermogravimetry (TG), differential thermogravimetry (DTG), differential thermal analysis (DTA), differential scanning calorimetry (DSC),[1–8] infrared spectroscopy,[9] and single-crystal X-ray diffraction,[10] and different types of water were identified in clinoptilolite.

Van Reenwiijk reported three endothermic DTA peaks for clinoptilolite. Based on the entropy values of water in the zeolite calculated from the DSC curves, at least three types of water were identified in the zeolite, including crystal water or low-entropy water, loosely bound water with high entropy, and zeolitic or high-entropy water.[8] Thermal and vacuum dehydration analysis of clinoptilolite-rich tuffs by DSC revealed the presence of three types of water as externally adsorbed, loosely bound zeolite, and tightly bound zeolite water and the heats of dehydration of each type of water were calculated as 54.4–65.8, 52.3–64.5, and 76.2–160 kJ/mol H_2O, respectively.[2]

Adsorption and desorption of water vapor on zeolites are reversible, i.e., the amount of heat required for desorption is equal to that released during adsorption. The application of zeolite for water adsorption is widely investigated for many purposes. Clinoptilolite and its Na, K, Ca, H, and NH_4 forms were tested for their applications in drying of air, hydrocarbons, H_2, etc.[4,11–13] Adsorption drying with zeolite was proposed as an alternative method to improve the energy efficiency of industrial drying.[14–18] The principle of zeolite drying is based on dehumidification of air before feeding to the dryer. At the same time, the air is preheated due to the release of adsorption heat, and the driving force for drying is increased. Zeolite 13X exhibited higher water adsorption capacity and better heat and mass transfer properties than pillared clays (PILCS), natural clay, and sand in immersion drying of wheat in an agitated particulate medium dryer.[14] It was shown that dryers using a zeolite air dehumidifier were more energy efficient than conventional dryers operating at moderate temperatures (52–70°C) in the food industry.[15] Zeolite was found to be more favorable than alumina-pillared clay for low drying temperatures (40–50°C) in multistage adsorption dryers with air dehumidification.[18] The two-stage dryer using zeolite for air dehumidification was found to be more

Correspondence: G. Narin, Department of Chemical Engineering, Usak University, 64200 Usak, Turkey; E-mail: guler.narin@usak.edu.tr

energy efficient than the one-stage system and current drying systems.[17] Local natural zeolite was proposed as a cheap substitute for expensive synthetic adsorbents also for industrial air drying applications.[19] Hydration and dehydration behaviors of local natural zeolites were investigated for drying and energy storage applications.[19–26] In such drying systems, the initial water content of the zeolite is important because it determines the adsorption capacity of the zeolite for water vapor. Based on the results of water vapor adsorption studies performed on an adsorbent bed, the local zeolite used in corn drying led to a significant increase in the drying rate and in the total amount of water desorbed for the same drying period. Furthermore, the heat released by the zeolite as it adsorbed water (100,000–2,500 J/g in the range of 0.01–0.115 g H_2O/g zeolite) was found to be higher than that absorbed by the corn during drying.[20] Heat of adsorption of water vapor in clinoptilolite-rich tuffs decreased from −64.1 to −47.7 kJ/mol H_2O as the solid moisture content increased from 4 to 11.5% (w/w).[24] The monolayer water vapor adsorption capacity was 9.68 g H_2O/g zeolite and the heat of adsorption values were reported as −65.4 and −32.7 kJ/mol H_2O for 1 and 5% (w/w) solid moisture contents, respectively.[26] Recently, Alver et al.[27] correlated the thermal behavior of clinoptilolite-rich natural zeolites from Turkey and their cation-exchanged forms to the size, particularly to the hydration energy, of the nonframework cations. The dehydration enthalpy change values were measured in the range of 9.84–14.60 kJ/mol H_2O by DSC.[27]

The thermal analysis techniques do not provide information about the state of the water molecules during dehydration of the zeolite. Infrared spectroscopic techniques are one of the methods that can be employed for this purpose.[9,28] Breger et al. distinguished between different types of water retained in clinoptilolite based on the infrared measurements and used the terms *loosely held* and *tightly bound* water to describe the types of water based on the intensities of 3410 and 3610 cm^{-1} bands, respectively.[9]

Temperature-programmed diffuse reflectance Fourier transform spectroscopy (TP-DRIFTS) allows analysis of the dehydration behavior of zeolites under similar conditions as in the thermal analysis methods. Beta et al. studied nonisothermal desorption of water on alkali-metal cation-exchanged X-type zeolites using TP-DRIFTS.[29]

In most adsorption and catalysis applications, H forms of zeolites are used. The H forms of zeolites are often prepared by thermal decomposition of their NH_4^+ forms. Kasture et al. showed that it was not possible to remove the ammonia from the NH_4-exchanged clinoptilolite by heating at 250°C and to transform the NH_4-clinoptilolite to the H form.[11] In infrared spectra of hydrated NH_4-exchanged zeolites, the changes observed in the OH stretching vibrations were attributed to the presence of the NH_4 groups and hydrogen bonds between the NH_4^+ and H_2O. The desorption profiles were obtained from the change in the area of the OH stretching band with temperature.[30] The mechanism of deammoniation consisted of thermal dissociation of NH_4^+ to NH_3 and a proton and diffusion of NH_3 out of the structure.[31]

Adsorption of gaseous ammonia has been employed in determination of acidity of zeolites. Adsorbed ammonia is coordinated on Brönsted acid sites (Si-OH-Al) in the protonated form of the zeolite (as NH_4^+ species; 1450 cm^{-1}) or coordinated as NH_3 species on the Lewis acid sites (1625 cm^{-1}). The latter band overlaps with bands of physisorbed water. Individual NH_4^+ (NH_3) sites in a zeolite show different vibrational activities due to their different local group symmetries. Diverse coordinations of NH_4^+ (monodendate, bidentate, tridentate) have been observed by infrared spectroscopy in a variety of zeolites.[32]

The aqueous ammonia solutions would also give information about the acidity of the zeolites. Thus, in this study, the effects of aqueous solutions of ammonia on a local clinoptilolite-rich zeolitic tuff are investigated. Natural, NH_4OH-treated, and subsequently calcined forms of the zeolitic tuff were characterized for this purpose. Moreover, dehydration behavior of a natural zeolite was investigated by TP-DRIFTS under vacuum for the first time. From the changes in the intensities of O−H and N−H bands upon heating under vacuum, the effects of the NH_4OH treatment and subsequent calcination on the dehydration behavior of the zeolite were examined.

MATERIALS AND METHODS

Preparation of Zeolite Samples

Clinoptilolite-rich natural zeolitic tuff mined from Gördes (Western Anatolia, Turkey) was crushed, washed with hot deionized water, fractionated by wet sieving using Retsch Test Sieves, and the fraction with particle diameter range of 38–45 μm was used in the experiments after drying at 110°C overnight in a static oven. This sample was labeled as NZ. Twenty-five grams of NZ was treated with 250 cm^3 of 2 mol/dm^3 aqueous ammonia solution, prepared from NH_4OH (Sigma-Aldrich 221228, ACS reagent, Germany), at 75°C for 5, 15, and 45 h on a magnetic stirrer (150 rpm). After the NH_4OH treatment, the particles were washed with excess deionized water and dried at 110°C overnight. These samples were labeled as NH_4-NZ-5h, NH_4-NZ-15h, and NH_4-NZ-45h, respectively. NH_4-NZ-15h was heated to 500°C in a static oven for 5 h and cooled to room temperature. The heating and cooling rates were 2°C/min. The sample obtained in this manner was labeled as H-NZ.

Characterization

Scanning Electron Microscopy

Particle and surface morphologies and crystal size and structures of the prepared samples were investigated by a

scanning electron microscope (SEM, XL-30S FEG, Philips, Eindhoven, The Netherlands). The particles were mounted directly on a carbon tape before analysis.

X-ray Powder Diffraction

The crystal mineral composition of NZ was determined by the qualitative X-ray powder diffraction analysis (XRD). The powder X-ray diffraction patterns of NZ, NH_4-NZ-15h, and H-NZ were recorded by a powder diffractometer (X'Pert Pro, Philips) equipped with an Ni-filtered CuK_α radiation source ($\lambda = 0.154056$ nm) over a 2θ range of 5° to 40° at a 10.15 s measurement time per step and a step size of 0.01671°. The X-ray source was operated at 40 mA and 45 kV. The sample preparation for the X-ray analysis involved gentle grinding of the particles into a fine powder using an agate mortar and pestle and packing of the powder into an aluminum sample holder with light compression to make it flat and tight.

Chemical Composition Analysis

The elemental compositions of NZ, NH_4-NZ-15h, and H-NZ were determined by an inductively coupled plasma–atomic emission spectrometer with axial plasma (ICP-AES; Liberty Series II, Varian, Victoria, Australia). The samples were treated with an alkali borate fusion flux (anhydrous lithium tetraborate, Fluka, Germany; zeolite in 10% w/w) and dissolved in 1.6 mol/dm^3 HNO_3 prior to analysis.

The elemental compositions were also analyzed via energy-dispersive X-ray spectroscopy (EDS) combined with the SEM. The zeolite powders were pelletized by pressing under 200 kPa pressure prior to the analyses. The EDS analyses were carried out on six randomly chosen regions on the surface of the pellets. The energy of the beam was 15 kV.

The carbon, hydrogen, and nitrogen contents of NZ and its NH_4OH treated and successively calcined forms (H-NZ) were determined by elemental analysis (Leco 932 CHNS, Leco Corporation, St. Joseph, MI).

Specific Surface Area and Pore Size

The pore volumes and surface areas of the samples were measured by volumetric N_2 adsorption–desorption at −196°C using an ASAP 2010 (Micromeritics Instrument Corp., Norcross, GA). Prior to the analyses, the samples were degassed in situ at 300°C for 24 h under 5×10^{-4} mbar.

Thermogravimetric Analysis

The changes in the mass of NZ, NH_4-NZ-15h and H-NZ upon heating were determined gravimetrically on a thermal gravimetric analyzer (TGA-51, Shimadzu, Kyoto, Japan) in the temperature range of 25–1000°C. The analyses were performed using approximately 10 mg samples, at a heating rate of 10°C/min and under 40 cm^3/min nitrogen flow. Prior to the analyses, the samples were hydrated on a saturated NH_4Cl solution having 75% relative humidity at 25°C in a desiccator for 2 weeks.

Differential Scanning Calorimetry

Differential scanning calorimetry was carried out by a Shimadzu differential scanning calorimeter (DSC-50, Shimadzu) in temperature range of 20–600°C under 40 cm^3/min nitrogen flow with a heating rate of 10°C/min. About 3.5 mg zeolite was used in the DSC analysis. The heat of adsorption values for the samples were calculated by integrating the DSC peaks.

Transmittance Fourier Transform Infrared Spectroscopy

Transmittance infrared spectra of NZ, NH_4-NZ-15h, and H-NZ were obtained by the standard potassium bromide (KBr) pellet method in the region of 400–4000 cm^{-1} after 40 scans at 4 cm^{-1} resolution at room temperature on a spectrometer equipped with a deuterated triglycine sulfate (DTGS) detector (FTS 3000 MX, Digilab Excalibur Series). Prior to the analyses, 1 mg of dehydrated zeolite samples was ground with 150 mg of KBr and the powder mixtures were pressed into pellets of 13 mm in diameter under 4 ton/cm^2 by a hydraulic press. The absorbance values were normalized with respect to the absorbance of the most intense band in the spectrum.

Temperature-Programmed Diffuse Reflectance Fourier Transform Infrared Spectroscopy

The dehydration behavior of the samples was determined by an in situ temperature-programmed diffuse reflectance Fourier transform infrared spectroscopy method. The samples were heated in situ from room temperature up to 520°C at a heating rate of 1°C/min under vacuum (10^{-6} mbar) in a praying mantis diffuse reflection attachment (Harrick Scientific Products Inc., Ossing, NY) equipped with a high-temperature, low-pressure reaction chamber (HVC-DRP, Harrick Scientific Products Inc.). The reaction chamber has two KBr windows and one glass window for observation. The temperature of the sample in the sample cup of the reaction chamber was measured by a K-type thermocouple and controlled by a low-voltage heating cartridge using a single-loop proportional-integral-derivative (PID) temperature controller (Series 989, Watlow, Winona, MN). The pressure in the chamber was measured by a Pirani vacuum gauge (measurement range: 5×10^{-4} to 1,000 mbar, Thermovac TR 216 S, Oerlikon Leybold, Cologne, Germany) and Penning vacuum gauge (measurement range: 10^{-9} to 10^{-3} mbar, PTR 225, Oerlikon Leybold). The zeolite powders were mixed with KBr in a ratio of 10% (w/w), ground together, and packed into the sample cup. The spectra were recorded at 50 scans at a resolution of 8 cm^{-1} in the 400–4000 cm^{-1} range after waiting for 15 min at each temperature. The background spectra were recorded using KBr. The spectra of the

samples were also taken after cooling to room temperature under vacuum and opened to the atmosphere after the dehydration experiment.

RESULTS AND DISCUSSION

Characterization

Scanning Electron Microscopy

From the scanning electron micrographs of NZ (a representative micrograph is shown in Fig. 1), it was observed that NZ is rich in clinoptilolite crystals with a tabular, coffin-like morphology with a characteristic monoclinic symmetry. Treatment with NH_4OH did not change the crystal morphology.

X-ray Powder Diffraction

The X-ray powder diffractograms of NZ, NH_4-NZ-15h, and subsequently calcined form (H-NZ) are shown in Fig. 2. In the X-ray diffractogram of NZ, the most intense peaks were detected at 9.87°, 22.41°, 26.05°, 28.17°, 30.09°, and 32.01° 2θ, which belong to the clinoptilolite phase. The qualitative mineralogical analysis revealed that the sample contained predominantly clinoptilolite (JCPDS 80-1557) as well as quartz (JCPDS 83-0540) and cristobalite (JCPDS 76-1390). It was revealed that the NH_4OH treatment and successive calcination at 500°C did not lead to significant changes in the diffraction angles, intensities, and widths of the characteristic peaks of clinoptilolite. The H-NZ was stable; that is, removal of the NH_3 from the structure did not lead to collapse of the crystal structure.

The nature, amount, and position of the extraframework cations in clinoptilolite channels affect the intensity of the peak corresponding to the (020) plane of clinoptilolite at 9.87° 2θ. The unchanged intensity of this band in the X-ray diffractogram of NH_4-NZ indicated that the cation composition of the zeolite did not change with the NH_4OH treatment.

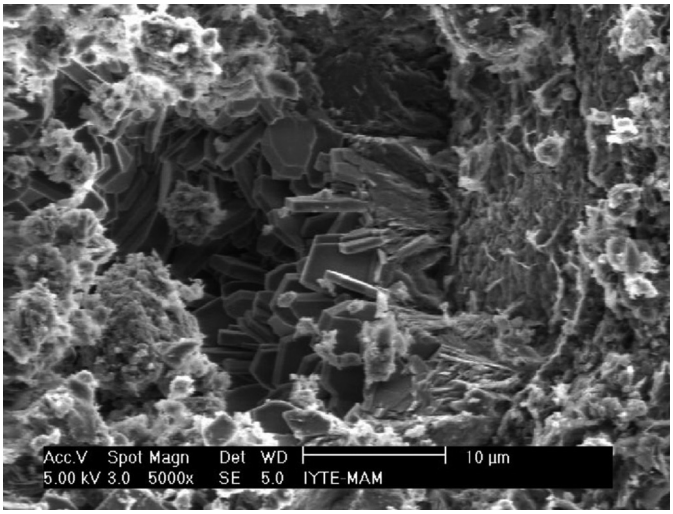

FIG. 1. Representative SEM micrograph of NZ (×5,000).

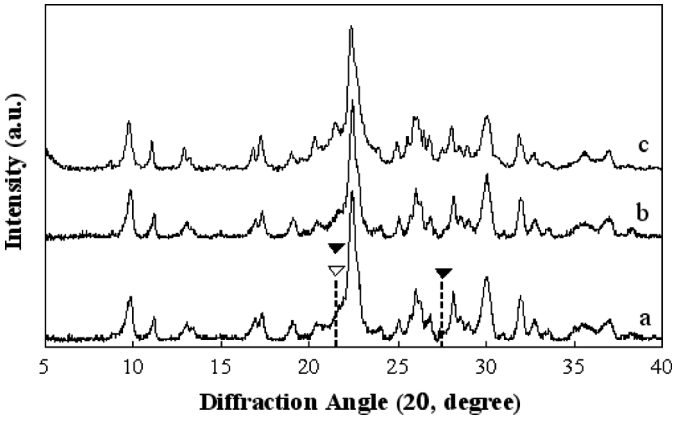

FIG. 2. X-ray powder diffractograms of (a) NZ, (b) NH_4-NZ-15h, and (c) H-NZ. ▼: quartz, ▽: cristobalite.

Chemical Composition

The chemical compositions of NZ, NH_4-NZ-15h, and H-NZ determined by ICP-AES and EDS are given in Table 1. It was revealed that NZ has an SiO_2/Al_2O_3 ratio of 6.46, which is typical for clinoptilolite.[4] The theoretical cation exchange capacity (TCEC) of NZ was calculated from the sum of the exchangeable cations (Ca^{2+}, Mg^{2+}, Na^+, and K^+) as 2.29 meq/g zeolite. The solid-phase chemical composition analysis revealed that the total cation content of NZ decreased only by 0.17 meq/g during the NH_4OH treatment, considerably lower than the TCEC, indicating that the reaction between the NZ and NH_4OH solution could not be explained solely by ion exchange.

The framework (Si and Al) and nonframework (Ca, Na, K, Mg) cation concentration of NZ did not change significantly with the contact period during the NH_4OH treatment. The changes in concentration of the species within the initial 5 h were more significant than those at later times. Thus, NH_4^+ exchange equilibrium was attained within the initial 5 h period.

The slight decrease in the concentrations of exchangeable cations in the zeolite with the ammonia treatment may be attributed to ion exchange and/or dissolution. However, no significant change was detected in the silicon and aluminum content of the zeolite with the NH_4OH treatment, implying lack of dissolution of the minor mineral phases accompanying the clinoptilolite. In highly basic solutions, as in the case here, OH^- ions in the solution may react with the clinoptilolite surface and caused the surface to be deprotonated[33]:

$$\equiv Si{-}OH + OH^- \rightleftharpoons \equiv Si{-}O^- + H_2O$$

The deprotonation of surface $\equiv$Si$-$OH groups leads to weakening of the Si$-$O$-$Si and Al$-$O$-$Si bonds on the

TABLE 1
Oxide compositions of NZ, NH_4-NZ, and H-NZ by EDS and ICP (% w/w)

	NZ		NH_4-NZ-5h		NH_4-NZ-15h		NH_4-NZ-45h		H-NZ	
Oxides	EDS	ICP	EDS	ICP	EDS	ICP	EDS	ICP	EDS	ICP
SiO_2	78.11	77.60	77.90	79.40	77.80	78.50	77.15	77.90	77.10	78.60
Al_2O_3	12.59	12.02	11.98	11.65	11.50	11.78	11.93	12.12	13.14	11.76
Na_2O	1.23	2.48	1.15	2.07	1.01	2.12	1.17	2.23	1.10	2.13
K_2O	3.24	3.78	3.02	3.34	3.60	3.45	3.41	3.61	3.14	3.55
CaO	3.99	3.30	4.33	2.74	4.86	3.56	5.26	3.50	3.80	3.41
MgO	1.34	0.02	1.60	0.02	1.25	0.02	1.09	0.02	1.90	0.02
MnO	—	0.71	—	0.74	—	0.68	—	0.65	—	0.56
SiO_2/Al_2O_3	6.20	6.46	6.50	6.82	6.76	6.65	6.46	6.42	5.86	6.68

surface and detachment of Si−OH. Those deprotonated surface groups (Si−O^-) behave as Lewis bases and the sorption of cations (M^{n+}) in the solution may lead to complex formation:

$$\equiv Si-O^- + M^{n+} \rightleftharpoons \equiv Si-OM$$

The adsorption of hydroxyl groups on the zeolite surface during treatment with basic solution has been also reported in the literature.[34]

The following equilibrium reactions may occur during the treatment of NZ with aqueous ammonia solution:

$$NH_3 + H_2O \rightleftharpoons NH_4OH$$

On the other hand, if the NH_4^+ is removed from the system by ion exchange, the equilibrium concentration of NH_4^+ will be maintained by ionization of NH_4OH according to the reaction given by:

$$NH_4OH \rightleftharpoons NH_4^+ + OH^-$$

$$NH_4^+ + A^+-NZ \rightleftharpoons NH_4^+-NZ + A^+$$

where A is an exchangeable cation in NZ.

Ammonium hydroxide could also react and neutralize acidic sites of the NZ giving NH_4–NZ:

$$NH_4OH + H_3O^+NZ \rightleftharpoons NH_4-NZ + 2H_2O$$

The equilibrium concentrations of NH_3 and NH_4^+ species in the solution depend on pH and temperature of the solution. At pH values above 9, most of the ammonium is found as NH_3.[4]

The chemical compositions determined by the CHN analysis are reported in Table 2 as CO_3^{2-}, H_2O, and NH_3. The acidic site concentration of NZ was calculated based on the amount of NH_3 adsorbed as 0.425 mmol/g zeolite. Indeed, a natural clinoptilolite from the Bigadiç region of Turkey was titrated with an organic base (diethyl amine) and 0.260–0.430 mmol diethyl amine was neutralized per gram of zeolite depending on the calcination time and temperature.[35] A very small amount of CO_3^{-2} ions (0.50–0.95%) was present in the samples under study. Ammonia-treated samples had higher CO_3^{-2} concentration due to adsorption of dissolved CO_2 from air by the aqueous ammonia solution.

Specific Surface Area and Pore Size

The N_2 adsorption–desorption isotherms for NZ and H-NZ are presented in Fig. 3, which correspond to Type IV according to IUPAC classification. The hysteresis loops that appeared in the multilayer range of the isotherms is usually associated with capillary condensation in mesopores (secondary porosity). Two types of porosity are present in clinoptilolite: the primary porosity (microporosity)

TABLE 2
CO_3^{2-}, H_2O, and NH_3 contents derived from CHN analysis (% w/w)

Species	NZ	NH_4-NZ-5h	NH_4-NZ-15h	NH_4-NZ-45h	H-NZ
CO_3^{2-}	0.50	0.95	0.70	0.80	0.60
H_2O	12.96	12.60	12.51	13.23	10.44
NH_3	0	0.59	0.57	0.61	0

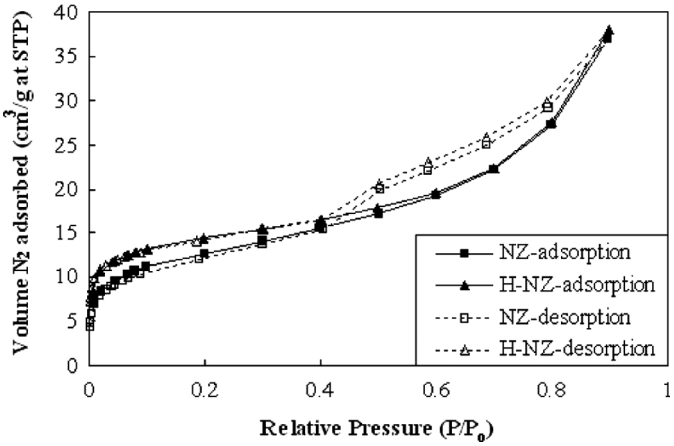

FIG. 3. N_2 adsorption and desorption isotherms determined volumetrically at −196°C.

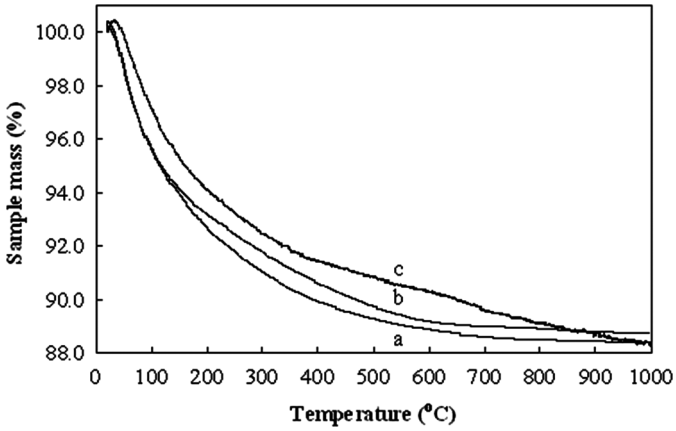

FIG. 4. TG curves for (a) NZ, (b) NH_4-NZ-15h, and (c) H-NZ.

results from the crystalline structure of the zeolite. The secondary porosity in the microporous solids is associated with the pores between the crystals and with the presence of the accompanying material in the tuff. The secondary porosity is usually presented by a system of mesopores and macropores.[4] Capillary condensation in the mesopores was observed at a relative pressure (P/P_o) of around 0.4 for both samples. The specific surface areas of NZ and H-NZ were calculated from the linear portion of the Brunauer-Emmett-Teller (BET) plots as 44 and 47 m^2/g, respectively. The average pore diameters ($4\,V/A_{BET}$) values were calculated as 4.3 nm for NZ and 5.0 nm for H-NZ. Because the BET model does not govern the micropore adsorption, the BET surface area was used for comparative purposes. Furthermore, N_2 molecules (kinetic diameter of 0.364 nm) cannot freely penetrate into the micropores of clinoptilolite. The NH_4OH treatment and successive calcination process caused a slight increase in the specific surface area and average pore size of NZ, which can be attributed to removal of the mineral impurities from the surface of NZ.

Thermogravimetric Analysis

The thermogravimetric (TG) curves for NZ and NH_4-NZ-15h are shown in Fig. 4. The continuous and uninterrupted TG curves indicated that the frameworks were not destroyed by heating up to 1000°C. The total amount of water loss up to 1000°C was determined as 11.6, 11.3, and 11.7% (w/w) for NZ, NH_4-NZ-15h, and H-NZ, respectively, indicating that the NH_4OH treatment and successive heat treatment had no significant effect on the water adsorption capacity of the zeolite except for differences in the water loss in certain temperature ranges.

When the H content determined by the elemental analyzer was converted to equivalent H_2O, it was nearly 12% (w/w) as given in Table 2. Thus, both TGA and elemental analysis gave consistent results for the H_2O content.

The TG curves showed that the weight loss occurred in a stepwise manner for all samples. In order to distinguish the different types of water present in the zeolites, the TG curves were analyzed according to the procedure outlined in the literature.[2] The low-temperature inflection point was observed at around 100°C for NZ. The rapid weight loss up to this temperature (4.4% w/w) was due to desorption of the externally adsorbed water. Another inflection point was detected at about 280°C for NZ and assigned to desorption of the loosely bound water (4.2% w/w). Above 280°C, slow desorption of the tightly bound water took place (2.9% w/w). The differences in the temperature of the inflection points from those reported in the literature can be attributed to the experimental conditions under which the dehydration was performed such as heating rate, atmosphere over the sample, preparation of the sample, and type of technique employed.[2]

The TG curve of NH_4-NZ-15h exhibited a different trend in the temperature range of 125–600°C. In this range, NH_4-NZ-15h lost less weight than NZ. It was not possible to observe two steps related to deammoniation and dehydroxylation during the thermal decomposition of NH_4-NZ-15h.

Differential Scanning Calorimetry

The DSC curves, with baseline drift subtracted, are shown in Fig. 5. In the DSC curve for NZ, two endothermic peaks were detected at 70 and 182°C. The other samples exhibited one endothermic peak at 70°C. These endothermic peaks were connected with elimination of the externally adsorbed water. The second endothermic peak in the DSC curve of NZ was attributed to desorption of the loosely bound zeolite water.[2]

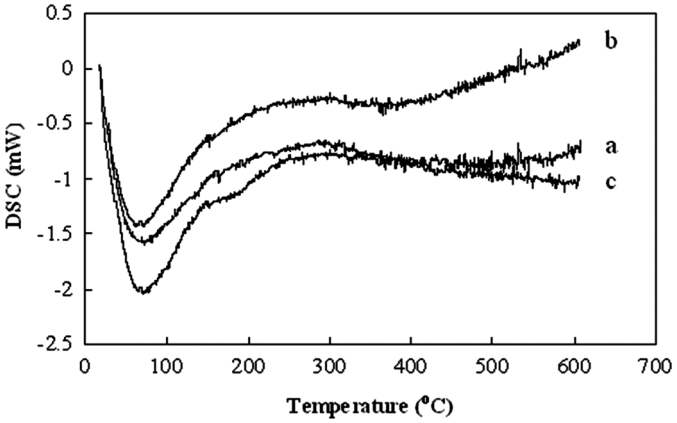

FIG. 5. DSC curves for (a) NZ, (b) NH4-NZ-15h, and (c) H-NZ.

Integrating the DSC peaks, the heats of dehydration values were calculated as 144, 74, and 170 kJ/mol H_2O for NZ, NH_4-NZ-15h, and H-NZ, respectively, and were found to be in agreement with the previously reported values,[2,25,26] but higher than those determined by DSC.[27] The DSC peaks were also integrated numerically in the temperature ranges of 25–100°C, 100–200°C, and 200–300°C in order to determine the heats of dehydration at different surface coverages. These heat values agreed well with the previously reported values determined by microcalorimetry.[25,26] The heats of dehydration values for NH_4-NZ-15h were lower than those for the other samples in all temperature ranges. The surface coverage values were determined based on the TGA data and change of the heats of dehydration with the surface coverage was shown in Fig. 6. The heats of dehydration decreased with the surface coverage for NZ and H-NZ as reported in the literature,[25,26] whereas it was almost independent of the surface coverage for NH_4-NZ-15h. This indicated that in DSC analysis of NH_4-NZ-15h, the enthalpy changes recorded were not due to endothermic dehydration but to some exothermic rearrangements in the structure occurring at high temperatures corresponding to removal of isolated OH groups. The decrease in the dehydration heat with the surface coverage could be explained by retention of water molecules more tightly by the cations at low surface coverages.[9]

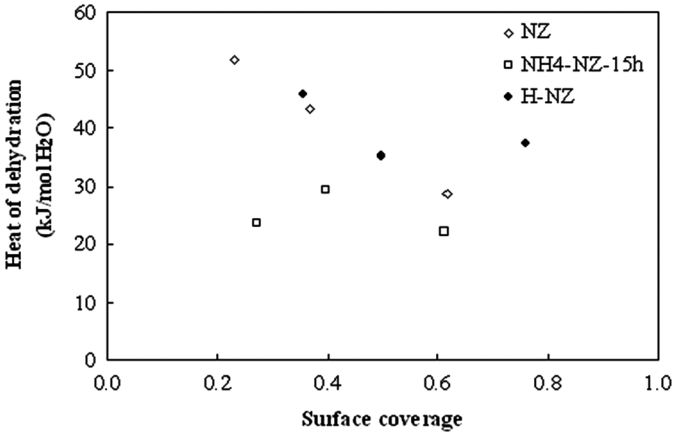

FIG. 6. Change of the heat of dehydration with surface coverage.

Transmittance Fourier Transform Infrared Spectroscopy

The transmittance infrared spectra of the samples recorded under atmospheric conditions are shown in Fig. 7. The bands detected in the range of 1200–400 cm^{-1} are assigned to the internal stretching vibrations of Si−O(Si) and Si−O(Al) in the tetrahedra. In this range bands were detected at 473, 530, 609, 677, 737, 795, and 1063 cm^{-1}. The strongest band appearing at 1063 cm^{-1} was attributed to asymmetric O-T-O stretching vibration. This band shifted to 1070 cm^{-1} for H-NZ, indicating distortion of the framework.

The intensity of the 473 cm^{-1} band is related to the nature and position of the cations in the zeolite structure. The comparison of the intensity of this band with those pseudo-lattice bands (500–700 cm^{-1}) is used to determine the degree of amorphization in zeolites. The band at 530 cm^{-1} is related to pore opening vibrations. This band could not have been detected in the spectrum of H-NZ. The band at 609 cm^{-1} is due to stretching of the internal tetrahedral bonds and is typical for the ordered crystal structure of clinoptilolite. The position of this band is related to the clinoptilolite content of the mineral. The intensity of this band in the spectrum of H-NZ decreased. The NH_4OH treatment and subsequent heating did not affect the band at 677 cm^{-1}. This band is due to symmetrical stretching vibrations of the Si−O bond existing in the 6-membered rings of the zeolite and is sensitive to changes in the type

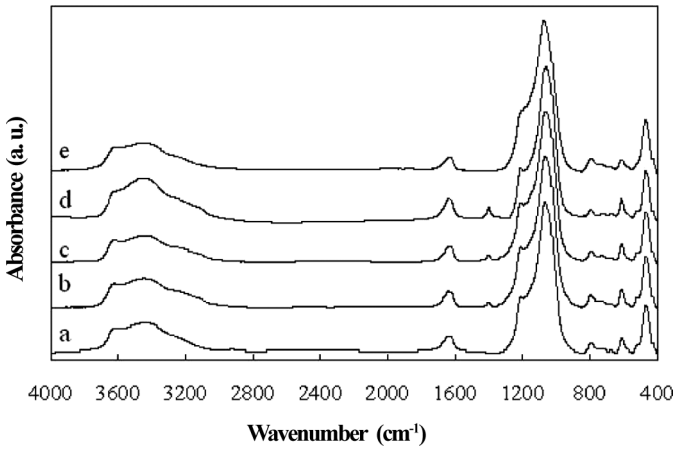

FIG. 7. Transmittance infrared spectra of the samples recorded under atmospheric conditions for (a) NZ, (b) NH_4-NZ-5h, (c) NH_4-NZ-15h, (d) NH_4-NZ-45h, and (e) H-NZ.

and amount of nontetrahedral cations. The bands at 737 and 795 cm^{-1} are due to vibrations of the Si−O−Al and Si−O−Si bonds, respectively. The shoulder at 1209 cm^{-1} is due to asymmetric stretching vibrations of T−O bonds. This band has become less prominent in the spectrum of H-NZ. The vibrations in the region 1600–3700 cm^{-1} are assigned to the presence of water. The isolated band at 1635 cm^{-1} is due to bending vibration of sorbed water. In the O−H stretching region (3000–3700 cm^{-1}), a broad band with two maxima at 3445 and 3620 cm^{-1} and a shoulder at 3250 cm^{-1} were detected related with stretching vibrations of hydroxyl groups. No remarkable changes were observed in either intensities or frequencies of the bands in the O−H stretching region upon the NH_4OH treatment and subsequent heating.

After the NH_4OH treatment, a new shoulder appeared at 3134 cm^{-1} and it was assigned to N-H stretching vibrations.[31] Also, an isolated band at 1402 cm^{-1} was detected in the spectrum after the NH_4OH treatment. Both bands disappeared after heating the sample at 500°C for 5 h. The band at 1402 cm^{-1} is close to the vibrations of the N-H bending centered at 1450 cm^{-1}. No significant change was observed in the intensity of the 3134 cm^{-1} band with the NH_4OH treatment period. The intensity of the 3445 cm^{-1} band inclined remarkably after the NH_4OH treatment for 45 h. This band is assigned to vibrations of the hydrogen bonds between water molecules and framework oxygen atoms.

The area of the 1402 cm^{-1} band increased proportionally with the NH_4OH treatment period (Table 3). On the other hand, the ammonia content of the NH_4-NZ samples, reported in Table 2, did not change significantly with the treatment period based on the CHN analysis,

Temperature-Programmed Diffuse Reflectance Fourier Transform Infrared Spectroscopy

The DRIFT spectra of NZ and its NH_4OH-treated and subsequently calcined forms recorded during in situ heating under vacuum are illustrated in Figs. 8–10, respectively. In the DRIFT spectra of the samples recorded at room temperature before vacuum, a broad band in the range of

TABLE 3
Area of 1402 cm^{-1} band for the sample treated for different periods with NH_4OH

Sample	NH_4OH treatment period (h)	1402 cm^{-1} band area
NZ	0	0
NH_4-NZ-5h	5	1.442
NH_4-NZ-15h	15	1.904
NH_4-NZ-45h	45	4.500

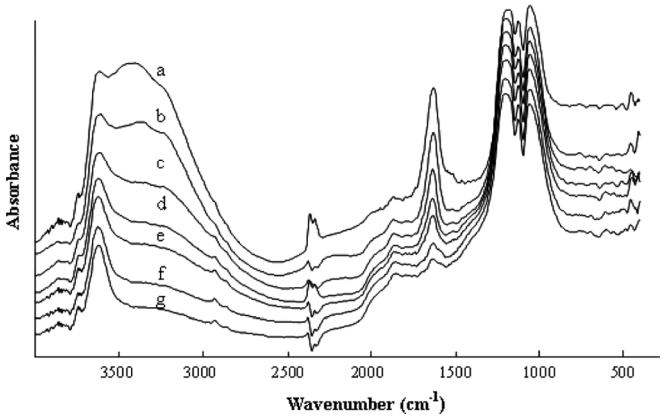

FIG. 8. DRIFT spectra for NZ: (a) before vacuum at 20°C, (b) under vacuum at 20°C, (c) at 132°C, (d) at 225°C, (e) at 301°C, (f) at 402°C; and (g) at 470°C.

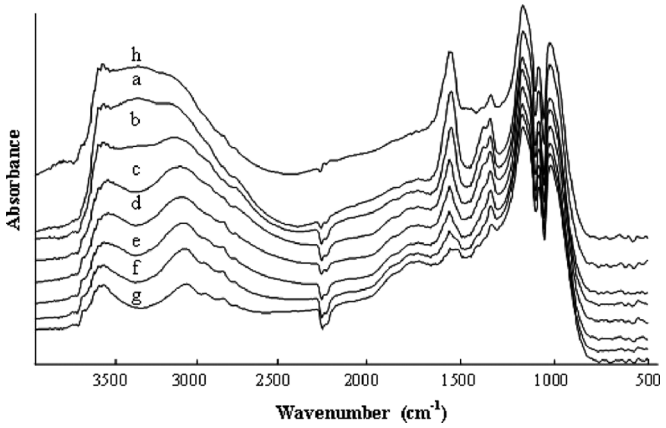

FIG. 9. DRIFT spectra for NH_4-NZ-15h: (a) efore vacuum at 24°C, (b) under vacuum at 24°C, (c) at 130°C, (d) at 230°C, (e) at 323°C, (f) at 410°C; (g) at 520°C, and (h) after open to the atmosphere at 24°C.

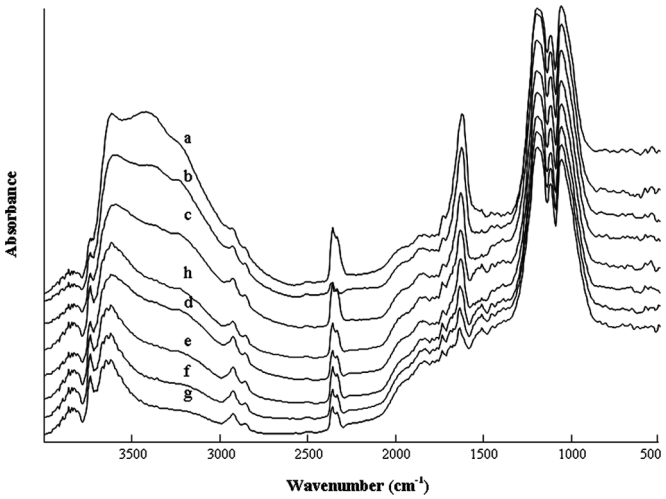

FIG. 10. DRIFT spectra for H-NZ: (a) before vacuum at 20°C, (b) under vacuum at 20°C, (c) at 120°C, (d) at 215°C, (e) at 305°C; (f) at 402°C; (g) at 487°C, and (h) at 150°C after heated to 487°C.

2500–3800 cm^{-1} was observed that was probably due to the abundance of water molecules present on the surface, which obscures the isolated OH stretching band.[13] Common bands were detected at 3610, 3410, 3230, 2920, 1630, 1200, 1140, and 1060 cm^{-1} in the spectra of the samples recorded under these conditions.

In the DRIFT spectra of NZ, the intensities and frequencies of the bands at 3850, 3750, 1890, and 2000 cm^{-1} did not change significantly with temperature. The band at 1510 cm^{-1} lost intensity with increase in the temperature and disappeared at 402°C. The band at 2920 cm^{-1} became more prominent as the temperature increased.

In the DRIFT spectrum of NH_4-NZ-15h recorded at room temperature, no bands were detected at 1510, 1890, 2000, 3750, and 3850 cm^{-1}. The bands at 1890 and 2000 cm^{-1} appeared as the temperature increased and disappeared from the spectra when the sample was opened to the atmosphere after heating. The 3750 cm^{-1} band became visible with the increase in temperature and remained in the spectrum after the sample was opened to the atmosphere. The bands at 1510 and 3850 cm^{-1} were detected after NH_4-NZ-15h was opened to the atmosphere after heating. The spectrum recorded after NH_4-NZ-15h was open to the atmosphere following heating at 520°C revealed that the dehydration of NH_4-NZ-15h was reversible and did not cause irreversible changes in the framework structure. NH_4-NZ-15h exhibited an extra band at 1402 cm^{-1} and two shoulders at 1450 and 3030 cm^{-1}. The band at 1450 cm^{-1} lost intensity with an increase in temperature and disappeared when the sample was heated to 520°C. The band at 1402 cm^{-1} was still detectable in the spectrum at 520°C and after the sample was opened to the atmosphere. The relative intensities of the 1402 and 1450 cm^{-1} bands decreased linearly with increasing temperature as shown in Fig. 11. The band at 3030 cm^{-1} lost intensity and became more prominent as the temperature increased.

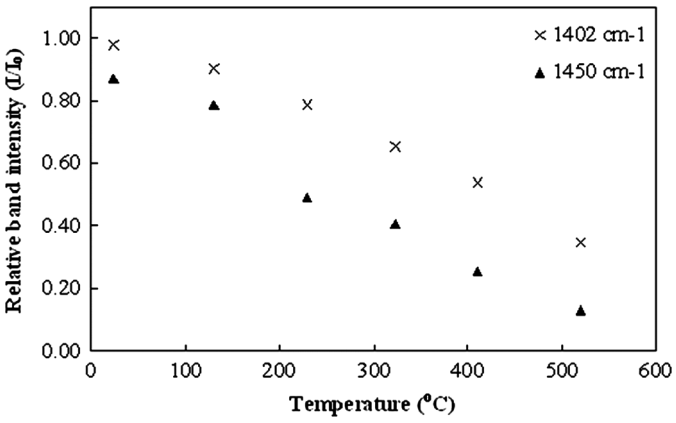

FIG. 11. Change in relative band intensities with temperature for NH_4-NZ-15h.

In contrast to the transmittance spectrum of NH_4-NZ-15h zeolite, the detection of the bands at 1402 and 3030 cm^{-1} in the spectrum after heating the sample to 520°C indicated that the ammonia could not have been removed after heating under vacuum. On the other hand, these bands were not detected in the spectra of H-NZ recorded at room temperature before the evacuation. This implied that the ammonia could be removed from NH_4-NZ-15h when the sample was heated in the presence of air and air is required to remove the ammonia from the structure.[36] Furthermore, because the sensor used to measure the temperature of the sample in the sample holder is located at the bottom of the holder, the temperature of the sample at the depth that the infrared (IR) beam can penetrate may not be as high as that measured at the bottom. Therefore, the ammonia present in the sample could not have been removed. In order to confirm this, NH_4-NZ-15h was removed from the sample holder after heating under vacuum and repacked in the holder and reanalyzed. In this case, the bands at 1402 and 3030 cm^{-1} were not detected.

In the DRIFT spectra of H-NZ, the band at 3850 cm^{-1} was not affected by temperature increase and evacuation. The band at 3750 cm^{-1} became more prominent as the temperature increased. This band is due to surface silanol (terminal) OH groups. The band at 2920 cm^{-1} was more significant in the spectrum of H-NZ recorded at room temperature before the evacuation compared to the other samples. The intensities and frequencies of the bands at 1890 and 2000 cm^{-1} did not change significantly with temperature. Different from NZ and NH_4-NZ-15h, an extra band at 1720 cm^{-1} was observed in the spectra of H-NZ at room temperature. Neither intensity nor frequency of this band changed significantly with temperature and evacuation. In the region of 1700–2200 cm^{-1}, overtone framework Si−O bands were observed in the IR spectrum of NH_4-analcime.[37]

Furthermore, a band appeared at 1510 cm^{-1} when H-NZ was heated to 402°C. The intensity or frequency of this band was not affected by a further increase in the temperature and continued to be detectable when H-NZ was cooled down to 150°C and opened to the atmosphere. This band could be due to the presence of carbonate ions in the tuff.

All samples exhibited common bands at 3610, 3410, 3230, and 1630 cm^{-1}, which are associated with water. The sharp band detected near 3610 cm^{-1} is assigned to typical stretching vibrations of isolated OH groups due to interaction of the hydroxyl of the water and the extraframework cations. The broad band at around 3410 cm^{-1} is characteristic for vibrations of OH groups bound to the framework oxygen atoms with hydrogen bonds. The band

at around 1630 cm^{-1} is assigned to the usual bending vibration of water.

At room temperature, before evacuation, the band at 3610 cm^{-1} appeared with single maximum in the spectra of NZ and H-NZ and with triple maxima in that of NH_4-NZ-15h (3650, 3610, 3590 cm^{-1}). The change in the shape of the 3610 cm^{-1} band detected in the spectra of NH_4-NZ-15h upon heating was found to be different from that for NZ. This band did not become as sharp upon heating as that for NZ. This might indicate the presence of different OH groups in NH_4-NZ-15h. During deammoniation of zeolite Y, the OH groups produced gave rise to two IR bands: one at 3640 cm^{-1}, referred to as the *high-frequency* (HF) *band*, and a second, *low-frequency* (LF) *band*, at 3540 cm^{-1}. These bands were attributed to the location of hydrogen atoms on two different oxygen atoms in the framework. The HF band was attributed to the H atom located within the large supercages and accessible to adsorbed molecules. The other H atom giving the LF band was less accessible and probably hidden within the β-cages of the structure.[34]

For NZ and H-NZ, the band at 3410 cm^{-1} shifted to 3350 cm^{-1} as the temperature increased and disappeared above 150°C. This shift can be attributed to an increase in the strength of the hydrogen bonds between water molecules and the framework oxygen atoms (due to a decrease in the distance between water molecules and the framework oxygen atoms). This band vanished from the spectrum of NH_4-NZ-15h after evacuation at room temperature but reappeared in the spectra at the same frequency after the sample was opened to the atmosphere subsequent to heating. This indicated that dehydration of this sample was reversible; that is, the framework did not collapse.

For NH_4-NZ-15h, the band at 3230 cm^{-1} showed a very different behavior upon heating compared to those in the spectra of NZ and H-NZ. In the spectrum of NH_4-NZ-15h, this band shifted to 3200 cm^{-1} when the sample was evacuated at room temperature. The band further shifted to lower wavenumbers when the temperature increased to 323°C. This shift indicated an increase in the bond strength with decreasing water content.[9] Above this temperature no change was observed in its position as its intensity continued to decline. The band turned to 3230 cm^{-1} after the sample was opened to the atmosphere. For NZ and H-NZ, the band at 3230 cm^{-1} lost intensity with an increase in the temperature without a change in its position.

For all samples, the relative intensities of the 1630, 3610, 3410, and 3230 cm^{-1} bands were found to decrease with increase in the temperature as shown in Fig. 12. The relative band intensity (I/I_o) was calculated by dividing the band intensity at each temperature by that in the spectrum of the zeolite at the fully hydrated state (I_o); that is, at room temperature, before evacuation.

The intensities of the bands at 1630 and 3410 cm^{-1} decreased in the same extent with temperature for all samples. This might means that these bands are related to water molecules bound to the zeolite in the same way. The former band was assigned to usual bending vibration of water. This band did not disappear even at 520°C under 10^{-6} mbar vacuum, indicating the presence of molecular water in the zeolite. The latter band was associated with the vibrations of OH groups bonded to the surface oxygen atoms via hydrogen bonds.[28] This band was assigned to loosely held water (H_2O^-)[9] and to vibration of the O−H···O bands.[38] It was reported that hydrogen bond strength of hydrogen-bonded OH groups varied with the surface coverage.[28]

The band at 3610 cm^{-1} declined in a more gradual manner with temperature compared to the other bands. Moreover, the samples exhibited different trends from each other regarding the decrease in the intensity of this band with temperature. This band was assigned to isolated OH stretching vibrations,[28] due to interaction of the hydroxyl of the water and the extraframework cations[34] and to tightly held water (H_2O^+).[9]

For NZ and H-NZ, the intensity of the band at 3230 cm^{-1} decreased with temperature in a trend similar to the other bands, whereas for NH_4-NZ-15h, its intensity declined more slowly. This band is in the region of stretching vibrations of OH groups.

For clinoptilolite, hydroxyl groups connected to the framework with chemical bonds are absent; thus, the hydroxyl groups are specific for water.[28] The vibrations in the 1600–3700 cm^{-1} region of the spectrum are due to presence of water in the zeolite. Within the zeolitic pores, the water molecules may interact with the extraframework cations (interaction of the lone pair electrons of the oxygen atom of water with the cations) via ion–dipole interaction with the zeolite framework (to the surface oxygen atoms) via hydrogen bonding and/or with the previously adsorbed water molecules.[28] In large-pore zeolites, all of the types of interactions mentioned above are possible. But in small-pore zeolites the water–water interactions are eliminated and thus the nearest neighbors for each water molecule are the cations and the surface oxygen atoms, for which the hydrogen bonding is weaker.[37,39] The interaction of water with the cations, if both hydrogens were left free, gives two sharp bands in the OH stretching region. The spectra that contain one sharp band together with a typical hydrogen-bonded band suggest a simultaneous adsorption of water via one set of lone-pair electrons to the exchangeable cation and via one hydrogen-to-surface oxygen atom, leaving the other hydrogen projecting freely into the cavity.[39] The interactions between the framework and the cations also impact the behavior of the water molecules in the pores of the zeolite.[28]

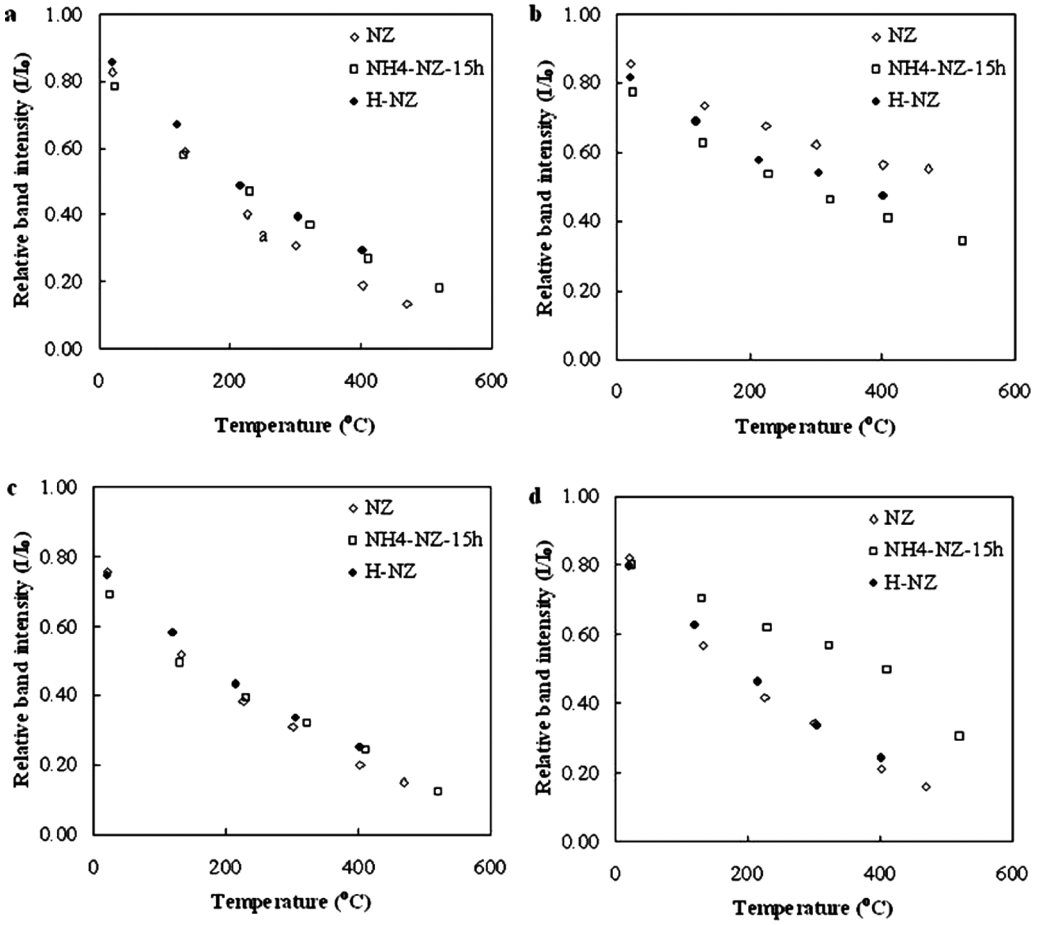

FIG. 12. Change in relative band intensities with temperature: (a) 1630 cm^{-1}, (b) 3610 cm^{-1}, (c) 3410 cm^{-1}, and (d) 3230 cm^{-1}.

The bands at 3610 and 3410 cm^{-1} could be regarded as corresponding to two different species of adsorbed water with slightly different hydrogen bonds.[9] These bands were assigned to the tightly bound and loosely held water in clinoptilolite, respectively. On the other hand, assignment of the bands in this way is contrary to that normally expected with the hydrogen bonding of water molecules where hydroxyl stretching frequencies normally decrease as bond strength increases.[9] At higher coverages, the free hydrogen would probably become increasingly bonded to adjacent water molecules and a greater proportion of the water would be hydrogen-bonded to the surface oxygen.[9] During dehydration, the hydrogen-bonded water molecules are converted to isolated OH groups. At low water content, the water molecules might be retained more tightly by the cations and the hydrogen bonds between the water molecules were lengthened (leading the hydrogen bond to become weaker).[9] Similarly, different retentions of water in heulandite were attributed to the cation-to-water bond distances[40] and to occupancy values of water molecules and a thermal parameter in clinoptilolite.[2] Higher occupancy values of water molecules and lower thermal parameters indicated stronger bonding.[2]

CONCLUSION

The zeolitic tuff used in the study was rich in clinoptilolite as shown by SEM and X-ray diffraction. Its SiO_2/Al_2O_3 ratio was 6.5 and did not change with the ammonia treatment. The chemical compositions of the natural, ammonia-treated, and successively calcined zeolites were nearly identical as determined by ICP and EDX analysis. Based on the CHN analysis, it was found that the natural zeolite adsorbed 0.425 mmol NH_3/g, indicating the concentration of the Brönsted acid sites. Thus, the zeolitic tuff investigated in the present study could be used as low-level Brönsted acid catalyst in heterogeneous reactions.

The relative intensities of the 1402 and 1450 cm^{-1} bands of NH_4-NZ-15h decreased linearly with increasing temperature, indicating that NH_3 was removed by heating the sample. The dehydration of the zeolitic tuff was reversible as shown by the DRIFTS studies. The desorption of the hydrogen-bonded water molecules occurred at lower

temperatures compared to the isolated OH groups, which could not be desorbed even at 520°C under 10^{-6} mbar vacuum.

The tuff adsorbed 12% (w/w) water vapor from air as understood by TGA analysis and elemental analysis. In the DSC curve of NZ, two endothermic peaks were detected at 70 and 182°C, whereas the other samples exhibited one endothermic peak at 70°C. The low-temperature peak was related with elimination of the externally adsorbed water, whereas the high-temperature peak was due to desorption of the loosely bound zeolite water. The heats of dehydration values calculated from the DSC peak areas were in agreement with the values in the literature. The heats of dehydration decreased with the surface coverage for NZ and H-NZ, whereas it was almost independent of the surface coverage for NH_4-NZ-15h. The decrease in the dehydration heat with the surface coverage was explained by tighter retention of water molecules by the cations at low surface coverages.

The changes in the state of different water molecules adsorbed in the zeolite during dehydration under vacuum were followed using DRIFTS. The heat of desorption values calculated based on the changes in the intensities of bands in DRIFT spectra with temperature allowed identification of different types of water molecules adsorbed in the zeolite. From the changes in the relative intensities of the bands associated with water as a function of temperature during the in situ dehydration, it was revealed that removal of the isolated OH groups requires higher heat compared to that for removal of the hydrogen-bonded OH groups. Because adsorption and desorption of water vapor in clinoptilolite are reversible processes, the heat absorbed during desorption would be released when water vapor was adsorbed in the samples. Thus, desorption with cheap and renewable energy sources such as solar energy and utilization of heat of adsorption in required places are possible with the zeolitic tuff. Around 900 J/g zeolite heat will be released to the surrounding by saturation of the dehydrated tuff with water vapor.

ACKNOWLEDGMENT

This study was financially supported by the State Planning Organization (project number: 98K122130). The authors thank Dr. A. Allahverdiev for his contribution to experimental work.

REFERENCES

1. Mumpton, F. Clinoptilolite redefined. American Mineralogist **1960**, *45*, 351–369.
2. Knowlton, G.D.; White, T.R.; McKague, H.L. Thermal study of types of water associated with clinoptilolite. Clays and Clay Minerals **1981**, *29*, 403–411.
3. Esenli, F.; Kumbasar, I. Thermal behaviour of heulandites and clinoptilolites of Western Anatolia. Studies in Surface Science and Catalysis **1994**, *84*, 645–651.
4. Tsitsishvilli, G.V.; Andronikashvilli, T.G.; Filizova, L.D.; Kirov, G.N. *Natural Zeolites*; Ellis Horwood: New York, 1992.
5. Shepard, A.O.; Starkey, H.C. The effects of exchanged cations on the thermal behavior of heulandite and clinoptilolite. In *Papers and Proceedings of the Fourth General Meeting*, Mineralogical Society of India, New Delhi, India, December 15–22, 1964; 155–158.
6. Carey, J.W.; Bish, D.L. Calorimetric measurement of the enthalpy of hydration of clinoptilolite. Clays and Clay Minerals **1997**, *45*, 826–833.
7. Bish, D.L. Thermal behaviour of natural zeolite. In *Occurrence, Properties, and Utilization of Natural Zeolites*; Ming, D.W.; Mumpton, F.A., Eds.; Brockport: New York, 1995; pp. 259–269.
8. Van Reenwiijk, L.P. The thermal dehydration of natural zeolites. Mededelingen Landbouwhogeschool Wageningen **1974**, *74*, 1–88.
9. Breger, I.A.; Chandler, J.C.; Zubovic, P. An infrared study of water in heulandite and clinoptilolite. American Mineralogist **1970**, *55*, 825–840.
10. Armbruster, T.; Gunter, M.E. Stepwise dehydration of heulandite-clinoptilolite from Succor Creek, Oregon, U.S.A.: A single-crystal X-ray study at 100 K. American Mineralogist **1991**, *76*, 1872–1883.
11. Kasture, M.W.; Joshi, P.N.; Soni, H.S.; Joshi, V.V.; Choudhari, A.L.; Shiralkar, V.P. Sorption properties of the natural, K, and partially deammoniated (H/NH_4) forms of clinoptilolite. Adsorption Science and Technology **1998**, *16*, 135–151.
12. White, D.A.; Bussey, R.L. Water sorption properties of modified clinoptilolite. Separation and Purification Technology **1997**, *11*, 137–141.
13. Rege, S.U.; Yang, R.T. A novel FTIR method for studying mixed gas adsorption at low concentrations: H_2O and CO_2 on NaX zeolite and γ-alumina. Chemical Engineering Science **2001**, *56*, 3781–3796.
14. Osorio-Revilla, G.; Gallardo-Velázquez, T.; López-Cortés, S.; Arellano-Cárdenas, S. Immersion drying of wheat using Al-PILC, zeolite, clay, and sand as particulate media. Drying Technology **2006**, *24*, 1033–1038.
15. Djaeni, M.; Bartels, P.V.; Sanders, J.P.M.; van Straten, G.; van Boxtel, A.J.B. Process integration for food drying with air dehumidified by zeolites. Drying Technology **2007**, *25*, 225–239.
16. Djaeni, M.; Bartels, P.V.; Sanders, J.P.M.; van Straten, G.; van Boxtel, A.J.B. Multistage zeolite drying for energy-efficient drying. Drying Technology **2007**, *25*, 1053–1067.
17. Djaeni, M.; Bartels, P.V.; van Asselt, C.J.; Sanders, J.P.M.; van Straten, G.; van Boxtel, A.J.B. Assessment of a two-stage zeolite dryer for energy-efficient drying. Drying Technology **2009**, *27*, 1205–1216.
18. Djaeni, M.; van Straten, G.; Bartels, P.V.; Sanders, J.P.M.; van Boxtel, A.J.B. Energy efficiency of multi-stage adsorption drying for low-temperature drying. Drying Technology **2009**, *27*, 555–564.
19. Ülkü, S.; Balköse, D.; Baltacıoğlu, H.; Özkan, F.; Yıldırım, A. Natural zeolites in air drying. Drying Technology **1992**, *10*, 475–490.
20. Ülkü, S.; Çakıcıoğlu, F. Energy recovery in drying applications. Renewable Energy **1991**, *1*, 695–698.
21. Ülkü, S. Adsorption heat pumps. Journal of Heat Recovery Systems **1986**, *6*, 277–284.
22. Tıhmınlıoğlu, F.; Ülkü, S. Use of clinoptilolite in ethanol dehydration. Separation Science and Technology **1996**, *31*, 2855–2865.
23. Çakıcıoğlu-Özkan, F.; Ülkü, S. The effect of HCl treatment on water vapor adsorption characteristics of clinoptilolite rich natural zeolite. Microporous and Mesoporous Materials **2005**, *77*, 47–53.
24. Çakıcıoğlu-Özkan, F.; Ülkü, S. Diffusion mechanism of water vapor in a zeolitic tuff rich in clinoptilolite. Journal of Thermal Analysis and Calorimetry **2008**, *94*, 699–702.
25. Ülkü, S. Natural zeolites in energy storage and heat pumps. Studies in Surface Science and Catalysis **1986**, *28*, 1047–1054.
26. Ülkü, S.; Balköse, D.; Alp, B. Dynamic heat of adsorption of water vapor on zeolitic tuff and zeolite 4A by flow microcalorimetry. Oxidation Communications **2006**, *29*, 204–215.
27. Alver, B.E.; Sakızcı, M.; Yörükoğulları, E. Investigation of clinoptilolite rich natural zeolites from Turkey: A combined XRF, TG/DTG,

DTA and DSC study. Journal of Thermal Analysis and Calorimetry **2010**, *100*, 19–26.
28. Bertsch, L.; Habgood, H.W. An infrared spectroscopic study of the adsorption of water and carbon dioxide by Linde molecular sieve X^1. Journal of Physical Chemistry **1963**, *67*, 1621–1628.
29. Beta, I.A.; Böhlig, H.; Hunger, B. Investigation of the non-isothermal water desorption on alkali-metal cation-exchanged X-type zeolites: A temperature-programmed diffuse reflection infrared Fourier transform spectroscopic (TP-DRIFTS) study. Thermochimica Acta **2000**, *361*, 61–68.
30. Sani, A.; Vezzalini, G.; Ciambelli, P.; Rapacciuolo, M.T. Crystal structure of hydrated and partially NH_4-exchanged heulandite. Microporous and Mesoporous Materials **1999**, *31*, 263–270.
31. Likhacheva, A. Yu.; Veniaminov, S.A.; Paukshtis, E.A. Thermal decomposition of NH_4-analcime. Physics and Chemistry of Minerals **2004**, *31*, 306–312.
32. Zecchina, A.; Marchese, L.; Bordiga, S.; Paze, C.; Gianotti, E. Vibrational spectroscopy of NH_4^+ ions in zeolitic materials: An IR study. Journal of Physical Chemistry B **1997**, *101*, 10128–10135.
33. Stumm, W.; Morgan, J.J. *Aquatic Chemistry: Chemical Equilibria and Rates in Natural Waters*, 3rd Ed.; Wiley: New York, 1996.
34. Breck, D.W. *Zeolite Molecular Sieves*; Wiley: New York, 1974.
35. Akpolat, O.; Gündüz, G.; Özkan, F.; Beşün, N. Isomerization of α-pinene over calcined natural zeolites. Applied Catalysis A: General **2004**, *265*, 11–22.
36. Tomazović, B.; Ćeranić, T.; Sijarić, G. The properties of the NH_4-clinoptilolite. Part 1. Zeolites **1996**, *16*, 301–308.
37. Likhacheva, A. Yu.; Paukshtis, E.A.; Seryotkin, Yu. V.; Shulgenko, S.G. IR spectroscopic characterization of NH_4-analcime. Physics and Chemistry of Minerals **2002**, *29*, 617–623.
38. Korkuna, O.; Leboda, R.; Skubiszewska-Zięba, J.; Vrublevska, T.; Gun'ko, V.M.; Ryczkowski, J. Structural and physicochemical properties of natural zeolites: Clinoptilolite and mordenite. Microporous and Mesoporous Materials **2006**, *87*, 243–254.
39. Crupi, V.; Longo, F.; Majolino, D.; Venuti, V. Vibrational properties of water molecules adsorbed in different zeolitic frameworks. Journal of Physics: Condensed Matter **2006**, *18*, 3563–3580.
40. Merkle, A.B.; Slaughter, M. Determination and refinement of the structure of heulandite. American Mineralogist **1968**, *53*, 1120–1138.